Cell Reports

Report

Progressive Aggregation of Alpha-Synuclein and Selective Degeneration of Lewy Inclusion-Bearing Neurons in a Mouse Model of Parkinsonism

Graphical Abstract

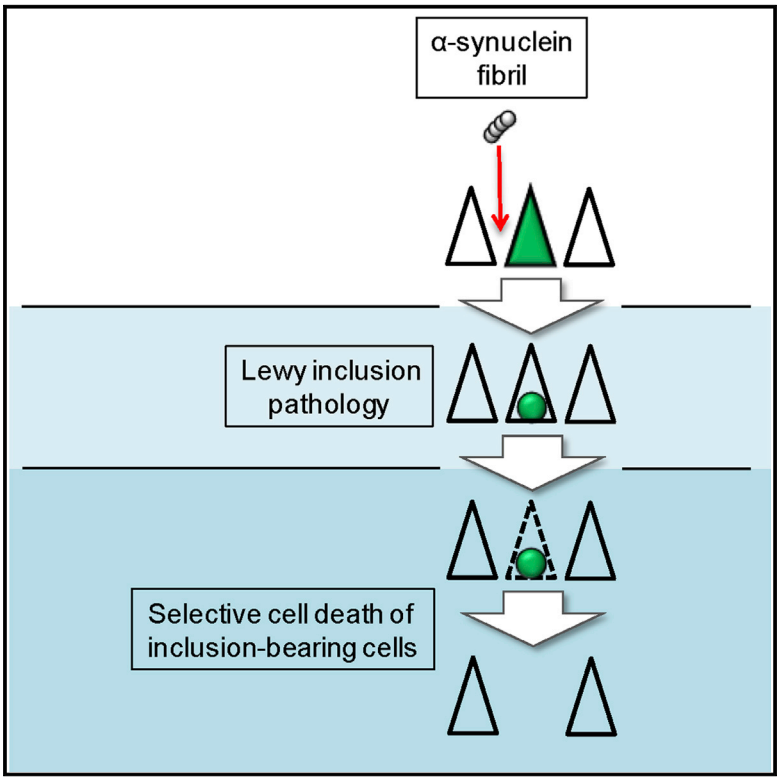

Highlights

- Alpha-synuclein fibrils seed conversion of endogenous protein into Lewy pathology
- Lewy inclusions undergo a stage-like compaction in vivo
- Lewy inclusion-bearing neurons selectively die, whereas non-bearing neurons survive

Authors

Valerie R. Osterberg, Kateri J. Spinelli, ..., Randall L. Woltjer, Vivek K. Unni

Correspondence

unni@ohsu.edu

In Brief

Lewy inclusions are the pathological hallmark of several forms of Parkinsonism and are found in regions where cell loss occurs. However, their relationship to cell death of inclusion-bearing versus non-bearing neurons is not known. Osterberg et al. use in vivo multiphoton imaging in a fibril-seeded mouse model to show selective cell death of inclusion-bearing neurons.

Osterberg et al., 2015, Cell Reports *10*, 1252–1260
March 3, 2015
http://dx.doi.org/10.1016/j.celrep.2015.01.060

CellPress

OPEN ACCESS
CellPress

Cell Reports
Report

Progressive Aggregation of Alpha-Synuclein and Selective Degeneration of Lewy Inclusion-Bearing Neurons in a Mouse Model of Parkinsonism

Valerie R. Osterberg,[1,5] Kateri J. Spinelli,[1,5] Leah J. Weston,[1] Kelvin C. Luk,[2] Randall L. Woltjer,[3] and Vivek K. Unni[1,4,*]
[1]Jungers Center for Neurosciences Research, Oregon Health and Science University, Portland, OR 97239, USA
[2]Department of Pathology and Laboratory Medicine, Institute on Aging and Center for Neurodegenerative Disease Research, University of Pennsylvania Perelman School of Medicine, Philadelphia, PA 19104, USA
[3]Department of Pathology, Oregon Health and Science University, Portland, OR 97239, USA
[4]Parkinson Center of Oregon, Department of Neurology, Oregon Health and Science University, Portland, OR 97239, USA
[5]Co-first author
*Correspondence: unni@ohsu.edu
http://dx.doi.org/10.1016/j.celrep.2015.01.060

SUMMARY

Aggregated alpha-synuclein inclusions are found where cell death occurs in several diseases, including Parkinson's disease, dementia with Lewy bodies, and multiple-system atrophy. However, the relationship between inclusion formation and an individual cell's fate has been difficult to study with conventional techniques. We developed a system that allows for in vivo imaging of the same neurons over months. We show that intracerebral injection of preformed fibrils of recombinant alpha-synuclein can seed aggregation of transgenically expressed and endogenous alpha-synuclein in neurons. Somatic inclusions undergo a stage-like maturation, with progressive compaction coinciding with decreased soluble somatic and nuclear alpha-synuclein. Mature inclusions bear the post-translational hallmarks of human Lewy pathology. Long-term imaging of inclusion-bearing neurons and neighboring neurons without inclusions demonstrates selective degeneration of inclusion-bearing cells. Our results indicate that inclusion formation is tightly correlated with cellular toxicity and that seeding may be a pathologically relevant mechanism of progressive neurodegeneration in many synucleinopathies.

INTRODUCTION

Evidence suggests that many neurodegenerative diseases involve spreading aggregation of specific proteins through the nervous system, potentially via a prion-like mechanism (for review, see Jucker and Walker, 2013, Guo and Lee, 2014, and Fraser, 2014). Synucleinopathies are such a group typified by pathologically aggregated alpha-synuclein in specific neuronal (e.g., Parkinson's disease and dementia with Lewy bodies) or glial (e.g., multiple-system atrophy) populations where cell loss occurs. Recent work demonstrates that aspects of progressive alpha-synuclein aggregation can be recapitulated in model systems by exogenous introduction of in-vitro-generated, preformed fibrils (PFFs) of alpha-synuclein (Volpicelli-Daley et al., 2011; Luk et al., 2012a, 2012b; Masuda-Suzukake et al., 2013; Sacino et al., 2014a, 2014b, 2014c). PFFs seed the aggregation of endogenous alpha-synuclein, and this aggregation spreads along synaptically connected pathways (Luk et al., 2012a, 2012b). One hypothesis is that this seeding involves a prion-like mechanism where introduced PFFs directly convert endogenous alpha-synuclein into an aggregated form that then propagates through the brain. However, recent work questions the ability of PFFs to cause widespread seeding of endogenous alpha-synuclein (Sacino et al., 2014a) and other potential mechanisms for spreading have been proposed (for review, see Brundin et al., 2008 and Golde et al., 2013). In addition, the role inclusion development plays in a cell's ultimate fate has been difficult to determine using current techniques. Evidence supporting either an association between Lewy pathology development and compromised cell health (Lu et al., 2005; Greffard et al., 2010) or the opposite, relative neuroprotection (Gertz et al., 1994; Bodner et al., 2006; Tanaka et al., 2004), exists in the literature.

To test these mechanisms in vivo, we developed a multiphoton imaging approach to monitor conversion of endogenous alpha-synuclein into pathologically aggregated states in living mouse brain after PFF injection. Transgenic mice expressing GFP-tagged wild-type (WT) human alpha-synuclein (Syn-GFP; Rockenstein et al., 2005) were injected with mouse sequence PFFs in primary sensory cortex and neuronal aggregation of Syn-GFP monitored in vivo using multiphoton microscopy. Serial imaging of individual mice allowed us to determine the time course and pattern of inclusion development up to 13 months after PFF injection. In vivo multiphoton fluorescence recovery after photobleaching (FRAP) experiments allowed us to measure alpha-synuclein mobility in different somatic pools and detected a slow alpha-synuclein turnover rate within inclusions. These data suggest that exogenously introduced PFFs convert endogenous alpha-synuclein into an aggregated state structurally

similar to inclusions found in human disease. Our data further suggest that aggregation is a stage-like process, with progressive compaction and coincident reduction in soluble cytoplasmic and nuclear levels as inclusions mature. Imaging of individual neurons over months detected selective cell death of inclusion-bearing neurons, suggesting a critical role for Lewy pathology in a cell's fate.

RESULTS

In Vivo Imaging Demonstrates a Stage-like, Progressive Maturation of Syn-GFP Inclusions within Neurons

PFFs were injected into right hemisphere sensory cortex of mice expressing Syn-GFP under control of the PDGF promoter. We placed cranial windows starting at 2 months post-injection. At this time point, the Syn-GFP expression pattern in neuronal cell bodies and presynaptic terminals in PFF-injected animals was unchanged from uninjected or PBS-injected controls (Figure 1A). Our previous work demonstrated that somatic Syn-GFP is not aggregated, does not spontaneously form inclusions, and is freely diffusible in the absence of PFF injection (Unni et al., 2010; Spinelli et al., 2014). Starting at ~2.5 months post-injection, Syn-GFP aggregates were readily apparent in neurites near the injection site and rarely in the contralateral hemisphere of PFF-injected mice (Figure 1B). At ~3 months post-injection, individual neurons near the injection site exhibited heterogeneous somatic Syn-GFP staining, with parts of the same cell body containing normal homogenous staining and other parts abnormal Syn-GFP accumulations (Figure 1B). At ~4–13 months post-injection, somatic inclusions increased in frequency near the injection site and took on a morphologically distinct character. Mature inclusions often presented as a cytoplasmic Syn-GFP accumulation ("body") with tendrils ("legs") that wrapped around the nucleus, giving mature inclusions a "spider-like" appearance (Figure 1B). Interestingly, unlike immature inclusions, at this later stage, there was a decrease in the normal-appearing soluble Syn-GFP staining in the cytoplasm and nucleus, compared to earlier time points (Figure 1B). Starting at ~4 months post-injection, mature inclusions were abundant in the contralateral left hemisphere as well (Figure 1B). Quantitative analysis of Syn-GFP homogeneity across cell bodies demonstrated a single population with low inhomogeneity in all neurons from uninjected and PBS-injected mice (Figure 1C). In contrast, PFF-injected mice at >3 months post-injection showed two distinct populations: one with low inhomogeneity (0.11 ± 0.03 inhomogeneity index; n = 56 cells/6 animals; Figure 1C) nearly identical to PBS-injected mice (0.10 ± 0.03 inhomogeneity index; n = 69 cells/2 animals; one-way ANOVA $p < 0.0001$; Tukey post hoc testing no significant difference for this comparison; Figure 1C) and a second population with a significantly higher inhomogeneity (0.47 ± 0.16; n = 108 cells/7 animals; Tukey post hoc test $p < 0.05$; Figure 1C), corresponding to neurons with spider-like inclusions (Figure 1C).

In Vivo Multiphoton FRAP Demonstrates Progressive Compaction of Syn-GFP Aggregates

Multiphoton FRAP can be used to measure Syn-GFP mobility of distinct pools in different subcellular compartments in vivo (Unni et al., 2010; Spinelli et al., 2014). We used this technique to first measure the somatic immobile Syn-GFP fraction in PBS-injected animals. All neurons demonstrated a low somatic immobile fraction (11% ± 7%; n = 7 cells/2 animals; Figure 2C), consistent with our previous work using in vivo multiphoton FRAP, Proteinase K digestion, and immunohistochemistry demonstrating no spontaneous somatic aggregation (Spinelli et al., 2014). We next performed FRAP on immature inclusions at ~3 months post-injection. Unlike in somata without aggregated Syn-GFP (in PBS-injected controls), we detected a large immobile fraction measured at 5 min post-bleach (70% ± 16%; n = 8 cells/3 animals; Figures 2A and 2C) that was significantly different than somata without inclusions (one-way ANOVA $p < 0.0001$; Tukey post hoc test $p < 0.05$; Figure 2C). In addition, simultaneous bleaching of aggregated and unaggregated regions in a single neuron demonstrated an immobile fraction only in the aggregated region of the soma (Figure 2A). Similar FRAP experiments performed in mature inclusions at ~4–13 months post-injection demonstrated an even larger immobile fraction (97% ± 6%; n = 16 cells/4 animals; Figures 2A and 2C), significantly different than both unaggregated regions and immature inclusions (one-way ANOVA $p < 0.0001$; Tukey post hoc test $p < 0.05$ for both comparisons; Figure 2C).

Chronic In Vivo Imaging Demonstrates a Low Molecular Turnover Rate within Aggregates

We extended the timescale of our FRAP experiments to determine whether the fraction of Syn-GFP that is immobile on the minutes timescale recovers over longer time scales. These results demonstrated that a partial Syn-GFP fluorescence recovery within the bleached region does occur over 7 days (immobile fraction 5 min: 97% ± 6%, n = 16 cells/4 animals; immobile fraction 7 days: 49% ± 17%, n = 10 cells/3 animals; one-way ANOVA $p < 0.0001$; Tukey post hoc test $p < 0.05$; Figures 2A–2C), corresponding to a 49% decrease in the previously immobile fraction. This indicates that there is a slow turnover of Syn-GFP within inclusions and that unbleached protein, either newly synthesized or from unbleached regions, moves into the bleached region and becomes incorporated over the course of several days.

Mature Somatic Inclusions Bear the Hallmarks of Human Lewy Pathology

Mice were sacrificed and brains fixed for immunohistochemistry at multiple time points following PFF injection. Starting at ~1 months post-injection, we detected abnormal Syn-GFP accumulations in cortical neuron cell bodies in the right (injected) hemisphere and neurites with an axonal appearance in cortical layers (V/VI), deeper than we can image in vivo, whereas similar accumulations were not seen in the cortex of PBS-injected or uninjected controls (data not shown), consistent with our in vivo imaging results (Figure 1) and our previous work (Spinelli et al., 2014). Starting at ~3 months post-injection, numerous inclusions were detectible (Figure 3) in more superficial layers (II/III), with the same mature, spider-like appearance imaged in vivo from these same cortical layers (Figure 1). These inclusions bore all the hallmarks of human Lewy pathology, including significant alpha-synuclein phosphorylation at serine-129 (Figures $3A_1$–$3A_4$, $3B_1$, and $3B_2$), amyloid dye binding (thioflavin S and X-34; Figures $3A_1$ and $3A_2$), and ubiquitination (Figure $3A_3$). Importantly, numerous

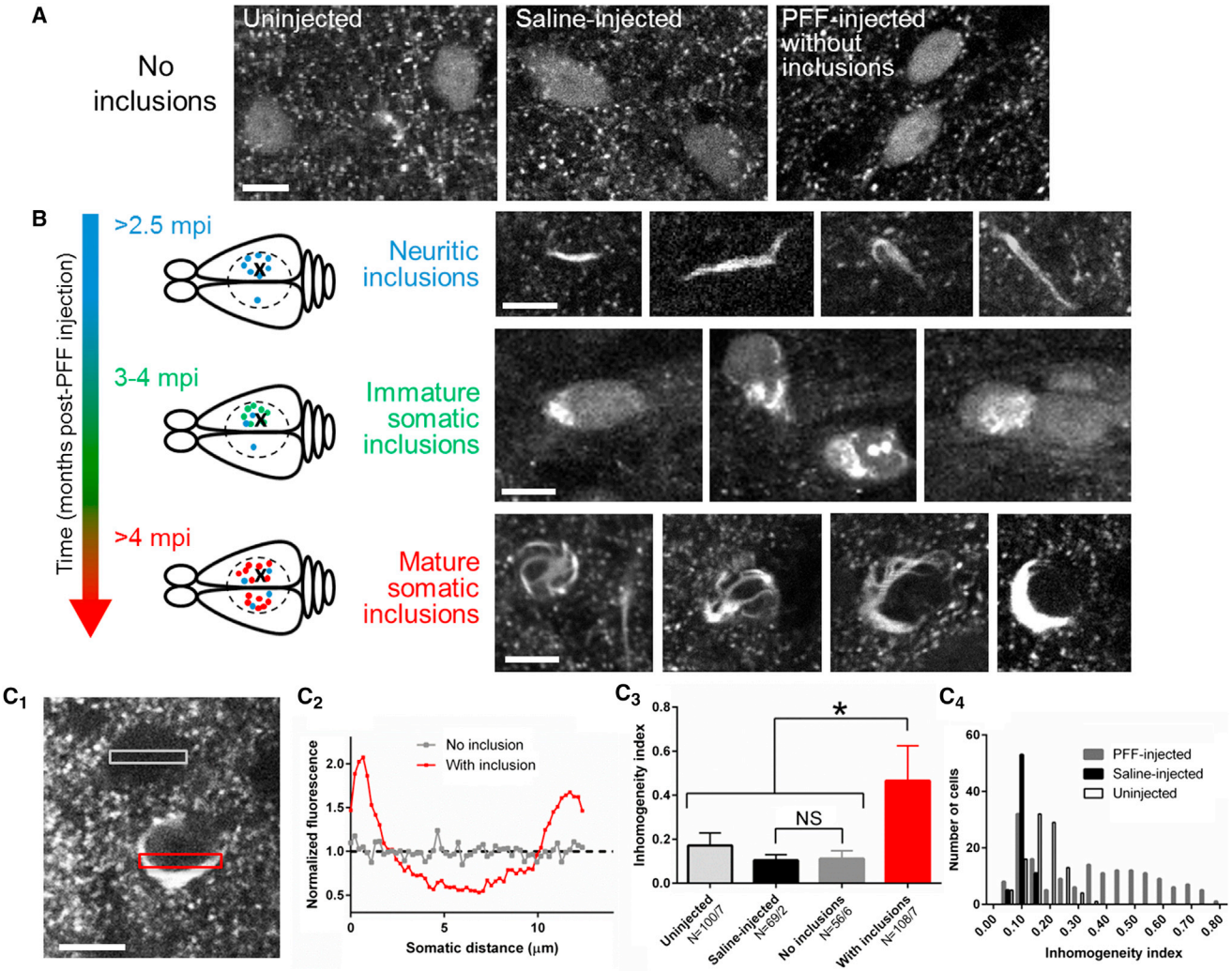

Figure 1. In Vivo Imaging Demonstrates a Stage-like, Progressive Maturation of Syn-GFP Inclusions within Neurons

(A) In vivo imaging in cortex layer II/III of uninjected (left), saline-injected (middle), or PFF-injected (right) animals at 2 months post-injection demonstrates punctate presynaptic staining within the neuropil and only homogenous somatic Syn-GFP staining within neurons. The scale bar represents 10 μm.

(B) Top: starting at 2.5 months post-injection, imaging near the PFF injection site demonstrates frequent neuritic Syn-GFP aggregates in layer II/III and rare neuritic aggregates in the contralateral hemisphere in the symmetric location to the injection. Schematic representation shows injection location in the right hemisphere (X), extent of cranial window (dashed circle), and location of neuritic aggregates (blue dot). The scale bar represents 10 μm. Middle: at 3 to 4 months post-injection, neurons (green dot in schematic) near the injection site began showing both disorganized somatic Syn-GFP inclusions and normal homogenous staining. The scale bar represents 10 μm. Bottom: at 4–13 months post-injection, only mature, organized somatic and neuritic Syn-GFP inclusions are present. Mature somatic inclusions have a stereotyped appearance, often with a single juxtanuclear accumulation and legs that wrap around the nucleus, giving a "spider-like" appearance. The normal homogenous somatic and nuclear Syn-GFP staining is absent in neurons containing mature inclusions. Schematic representation shows location of numerous mature somatic inclusions (red dot) near the injection site and in the contralateral hemisphere. The scale bar represents 10 μm.

(C) Example of two neurons (C_1), one with normal homogeneous staining and one with a mature inclusion, and transect ROIs used to measure fluorescence (C_2) across the cell body. An inhomogeneity index was calculated (see Experimental Procedures) and used to measure the mean index value (C_3) in neurons from uninjected, saline-injected, and PFF-injected animals with and without inclusions. Neurons from uninjected, saline-injected, and PFF-injected animals without inclusions show low levels of inhomogeneity, whereas inclusion-bearing neurons from PFF-injected animals were significantly more inhomogeneous. n = cells/animals. Histogram of inhomogeneity index values from cells from all three groups (C_4) shows single populations with low inhomogeneity in uninjected and saline-injected animals, whereas PFF-injected animals show two distinct populations: a low-index one nearly identical to saline-injected animals and a high-index population corresponding to neurons with mature somatic inclusions. The scale bar represents 10 μm. All error bars show SD.

similar inclusions composed only of untagged endogenous mouse alpha-synuclein with the same morphology and staining characteristics (Figure 3A_5) were found in nearby Syn-GFP-negative cells, strongly suggesting that the GFP tag does not interfere with the mechanism of Lewy pathology formation. Staining with an anti-GFP antibody demonstrated that the green fluorescent inclusions were made of Syn-GFP and not an endogenous, green autofluorescent species or autofluorescence from the injected

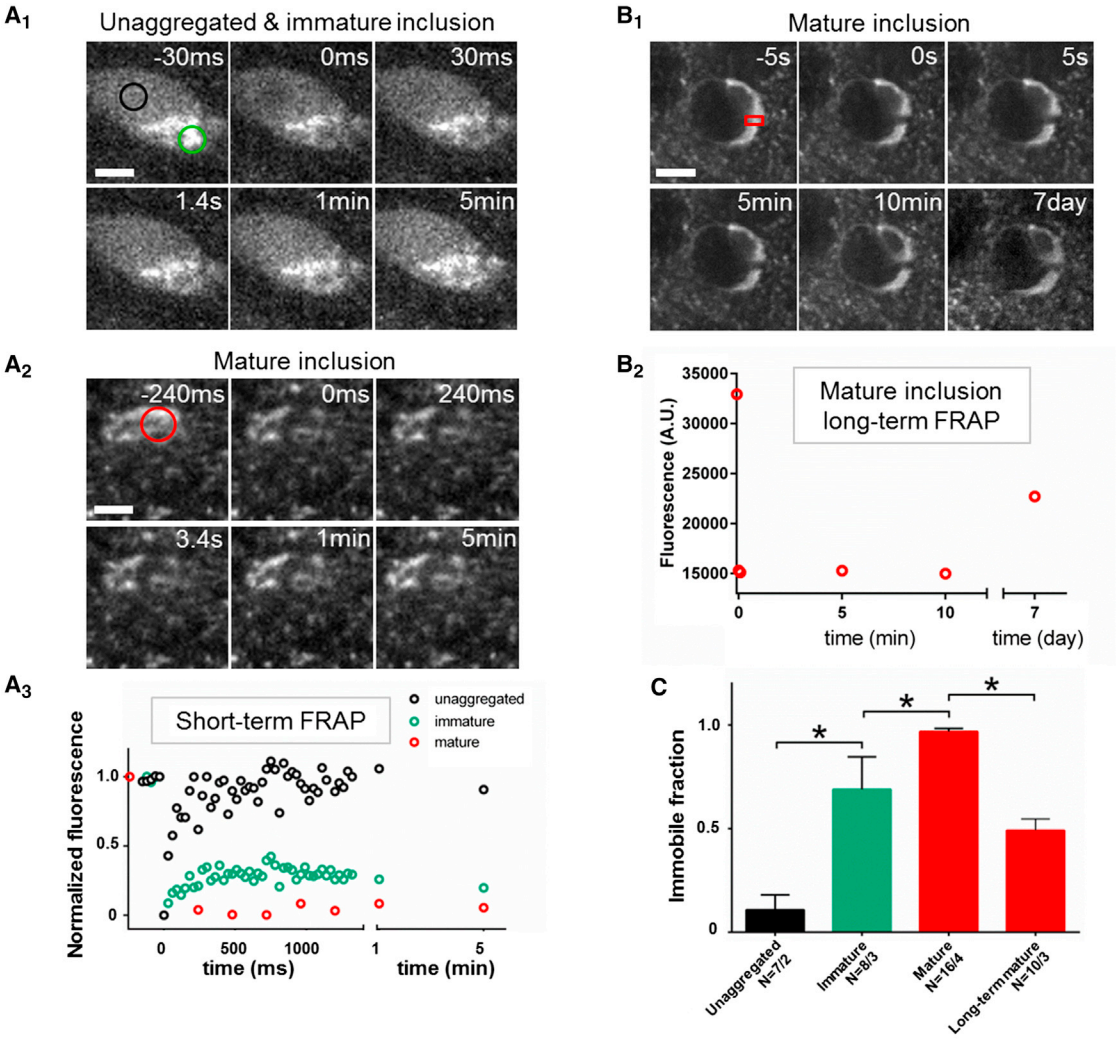

Figure 2. In Vivo FRAP Demonstrates Progressive Compaction of and a Low Molecular Turnover Rate within Syn-GFP Inclusions

(A) Individual neuron (A_1) with an immature inclusion at 3 months post-injection demonstrates mixed aggregated and unaggregated somatic Syn-GFP staining pattern. Two ROIs, one within (green circle) and one outside (black circle) the aggregated portion, are photobleached simultaneously and sequential images shown before and after FRAP. Bleach pulse occurs just before time 0. The scale bar represents 5 μm. Similar FRAP experiment of the aggregated portion (red circle) of a mature inclusion (A_2) at >4 months post-injection. The scale bar represents 5 μm. Mean fluorescence intensity (A_3) from the three ROIs from the two cells in (A_1) and (A_2) plotted on the same timescale demonstrates complete recovery back to baseline of the homogeneous staining but large immobile fractions in the immature and mature inclusions.

(B) Individual neuron (B_1) with a mature somatic inclusion at 4 months post-injection and absent unaggregated Syn-GFP staining in the remaining cytoplasm or nucleus. ROI (red rectangle) shows part of inclusion that was photobleached. The scale bar represents 7 μm. Mean intensity from this ROI over time (B_2) shows a large immobile fraction at 5–10 min post-bleach, which recovers substantially at 7 days post-bleach.

(C) Group data comparing measured immobile fractions from unaggregated somatic Syn-GFP, immature and mature inclusions at 5 min post-bleach, and mature inclusions 7 days post-bleach, showing a significant progressive increase in the immobile fraction from immature to mature inclusions as measured at 5 min. At 7 days post-bleach, however, 49% of the previously immobile fraction recovers, demonstrating a slow turnover of protein within inclusions. n = cells/animals. All error bars show SD.

material itself (Figures 3A_4 and 3B_1). Further evidence for this came from PFF injections in non-transgenic animals, which did not exhibit any green fluorescent inclusions (Figure S1), also demonstrating that the Lewy pathology we image in vivo and in fixed tissue is composed of Syn-GFP and not autofluorescent species. Quantification of Syn-GFP levels within inclusions versus neighboring Syn-GFP-positive neurons without inclusions demonstrated a significant, large increase in Syn-GFP protein within mature Lewy inclusions (17 ± 11-fold increase; n = 25 cell pairs/3 animals; $p < 0.0001$; paired t test; Figure 3B). Syn-GFP within inclusions was also significantly more colocalized with phospho-synuclein forms than Syn-GFP in cells without inclusions (average Pearson's coefficient within inclusions: 0.66 ± 0.19, n = 22 cells/3 animals; without inclusions: 0.03 ± 0.02,

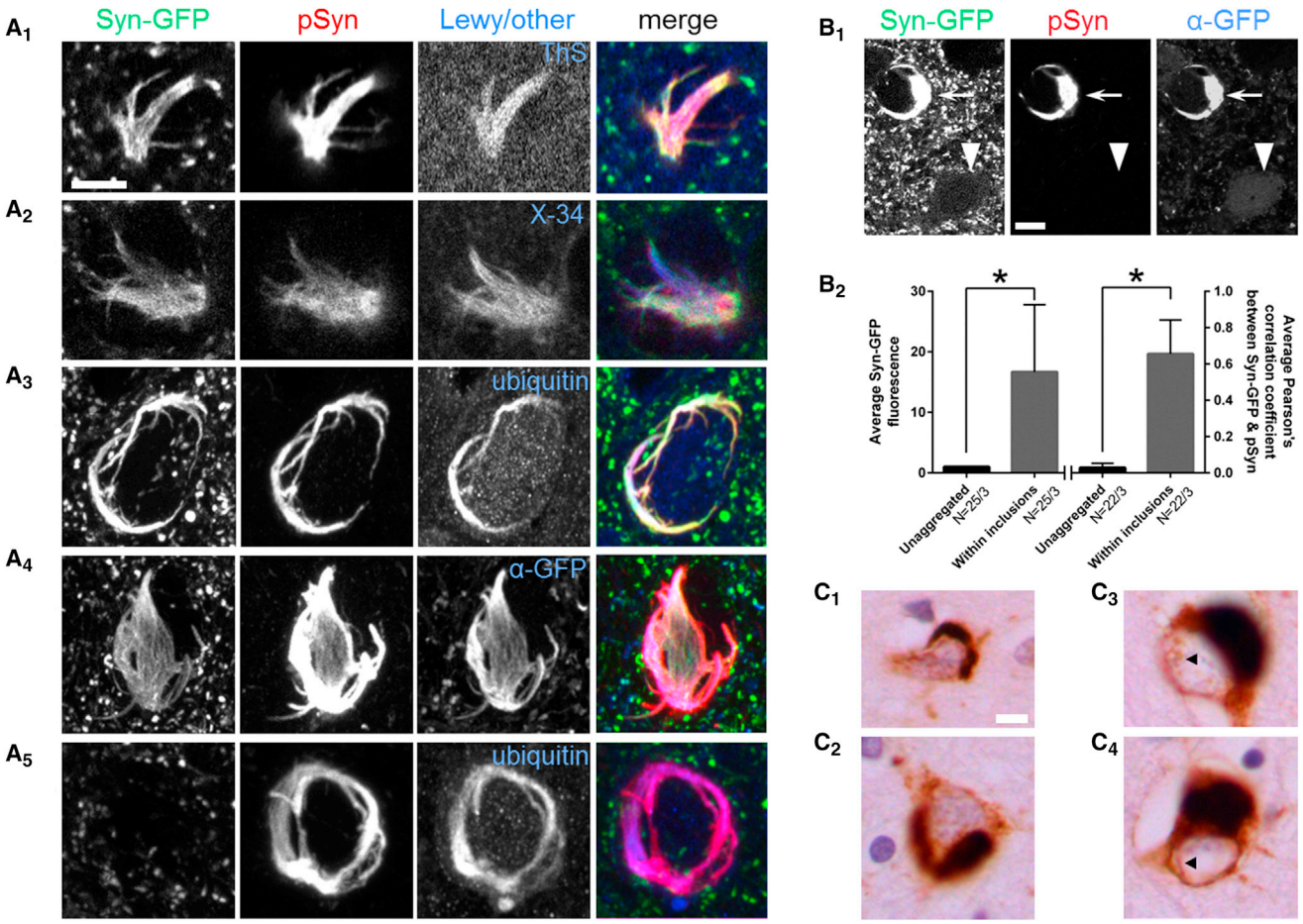

Figure 3. Mature Somatic Inclusions Bear the Hallmarks of Human Lewy Pathology

(A) Mature Syn-GFP inclusions are heavily phosphorylated at serine-129 (A_1–A_4), in an amyloid dye binding configuration (A_1 and A_2) and ubiquitinated (A_3). The green fluorescence from these inclusions is due to the presence of Syn-GFP and not an endogenous autofluorescent species, because they colabel with antibody to GFP (A_4). Similar mature inclusions made only of untagged endogenous mouse alpha-synuclein (A_5) are also present in nearby neurons that do not express Syn-GFP. These inclusions share a similar morphology and modification state to Syn-GFP-positive ones. Syn-GFP levels within mature inclusions (B, arrow) are greatly increased over levels of the protein in nearby neurons without inclusions (arrowhead). Colocalization of Syn-GFP with serine-129 phosphorylated alpha-synuclein (B) is also increased in inclusions versus cells without inclusions. n = cells/animals.

(C) Individual neurons from human frontal cortex in cases of dementia with Lewy bodies (C) are stained with hematoxylin to outline the nuclei in blue and for serine-129 phospho-synuclein aggregates in brown. Two examples demonstrate wrapping of aggregated alpha-synuclein around the nucleus (C_1 and C_2), similar to that seen in mature mouse inclusions. Two other examples show "legs" of the inclusion that wrap around the nucleus (C_3 and C_4, black arrowhead), also similar to mature mouse inclusions.

The scale bar represents 5 μm. See also Figures S1 and S2. All error bars show SD.

n = 22 cells/3 animals; $p < 0.0001$; t test; Figure 3B). Sagittal sections of the injected right hemisphere also demonstrated the presence of cortical and hippocampal inclusions, composed either of Syn-GFP or endogenous mouse alpha-synuclein, at and distant to the injection site along the anterior-posterior axis of the cortex (Figure S2).

Aggregated Cortical Alpha-Synuclein Pathology in Human Dementia with Lewy Bodies Cases Is Structurally Similar to Mature Mouse Aggregates Imaged In Vivo

Review of alpha-synuclein inclusion pathology stained for serine-129 phospho-forms in frontal cortex in three cases of dementia with Lewy bodies revealed numerous somatic inclusions that wrapped around the nucleus with a similar morphology to what we observe with our Syn-GFP inclusions in vivo (Figures 3C_1 and 3C_2). No staining was seen in a review of three age-matched control cases without clinical evidence of dementia (data not shown). In addition, frequent cortical inclusions were found with tendrils of aggregated alpha-synuclein wrapping around the nucleus (Figures 3C_3 and 3C_4), again similar to our mature Syn-GFP inclusions in mice.

Selective Degeneration of Inclusion-Bearing Neurons

Serial imaging of individual inclusion-bearing and non inclusion-bearing neurons over the course of 7 months detected a high

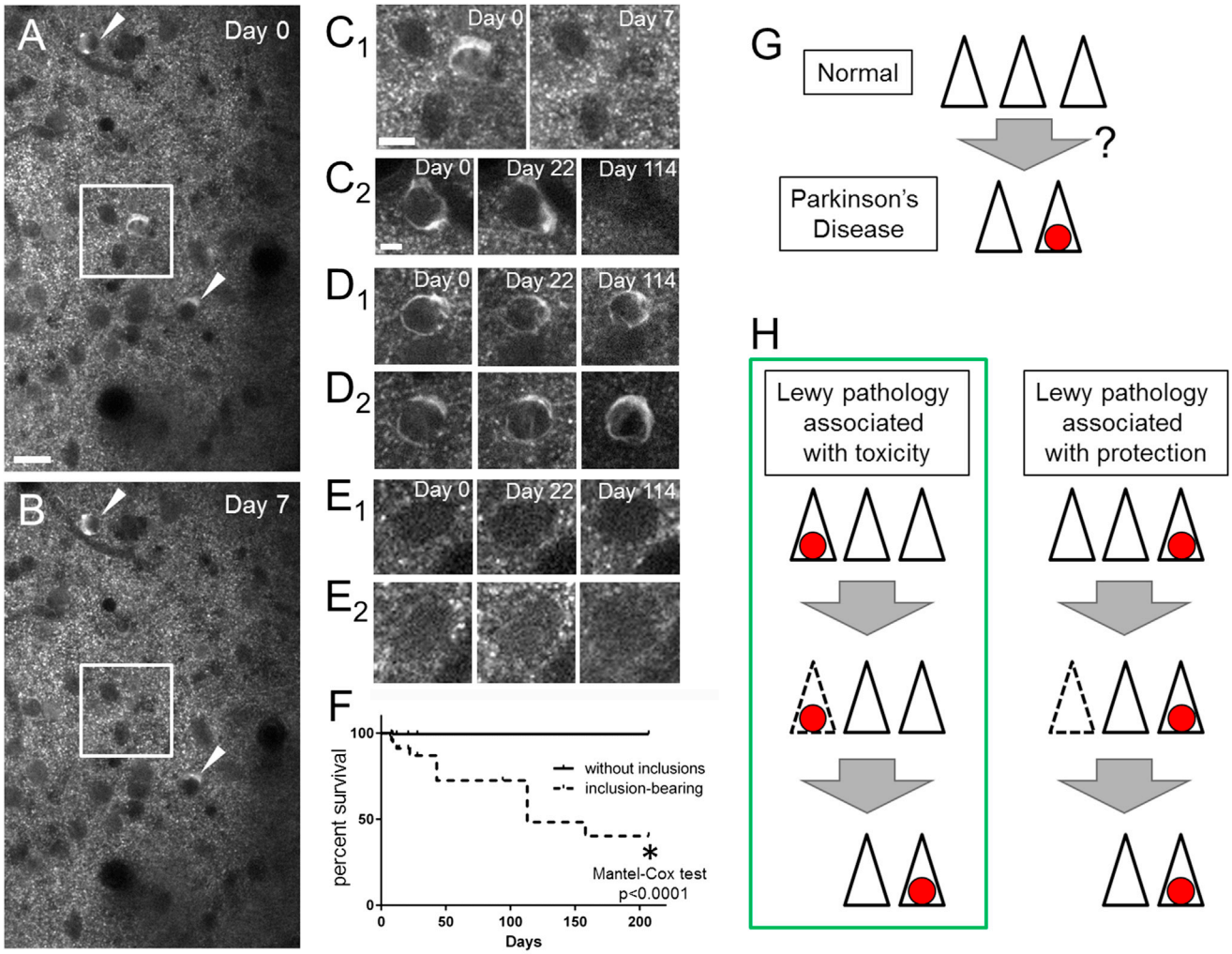

Figure 4. Chronic In Vivo Imaging Demonstrates Selective Degeneration of Inclusion-Bearing Neurons

(A and B) Field of neurons imaged 1 week apart demonstrate blood vessels by their negative stain, multiple neurons without inclusions, and three mature inclusion-bearing neurons (white square and arrowhead) on day 0. The scale bar represents 20 μm.

(C–E) One of these neurons (white square) degenerates by day 7 and is shown at higher power (C_1). The scale bar in (C_1) represents 10 μm and in (C_2)–(E_2) represents 5 μm. Chronic imaging of individual neurons over months shows degeneration of some inclusion-bearing cells (C) with persistence of other cells with (D) and without (E) inclusions.

(F–H) Group data (F) show selective degeneration of inclusion-bearing neurons over 7 months. Schematic showing the loss of neurons in brain regions affected by Parkinson's disease with the presence of Lewy pathology (red circle) in some of the remaining cells (G) and two different models for how this same final state might arise (H). One model posits a positive correlation between Lewy pathology presence and cell death, whereas the other an inverse correlation.

rate of disappearance of mature Lewy inclusion-bearing cells (40.3% survival at 207 days; n = 154 cells/4 animals; Figures 4A–4D). In contrast, adjacent neurons without inclusions had a very low rate of disappearance (99.4% survival at 207 days; n = 272 cells/4 animals; Figures 4A, 4B, and 4E). This is similar to our previous work demonstrating an undetectable rate of loss of Syn-GFP-expressing neurons (100% survival of 42 cells) in uninjected animals over 49 days (Unni et al., 2010). Survival analysis showed that the presence of mature inclusions was strongly correlated with cell death in the bearing neurons, with a median survival of 113 days ($p < 0.0001$; Mantel-Cox test; Figure 4F). In addition, we did not detect large-scale changes in the shape of inclusions, even if they persisted for several months (Figure 4D).

DISCUSSION

We have shown that the intracortical injection of mouse WT alpha-synuclein PFFs into mice expressing human WT alpha-synuclein tagged with GFP leads to the conversion of the transgenically expressed protein into neuritic and somatic inclusions that bear the hallmarks of human Lewy pathology. Previous work has questioned whether PFFs can seed widespread conversion of alpha-synuclein into an aggregated form when it does not

contain the A53T point mutation (Sacino et al., 2014a). Specifically, cross-reactivity between phospho-serine-129 synuclein antibodies and neurofilament-L was suggested as the source of signal interpreted as alpha-synuclein aggregates in other experiments. In this work (Sacino et al., 2014a), alpha-synuclein aggregates were only seen distant from injection site in animals expressing the A53T point mutant, although more recent work from the same group does show some evidence of spreading human WT alpha-synuclein aggregation (Sacino et al., 2014c). Our work uses a parallel approach to detect aggregated alpha-synuclein based on endogenous GFP fluorescence. Both in fixed tissue and with in vivo multiphoton imaging, we detect a time-dependent, progressive aggregation of WT human Syn-GFP only after PFF injection and not in controls. In addition, injections localized to sensory cortex in one hemisphere produced a clear spread of aggregation to the contralateral sensory cortex ~3 to 4 months post-injection. These results, taken together with previous work (Luk et al., 2012a, 2012b; Masuda-Suzukake et al., 2013), suggest that PFFs can seed progressive aggregation of endogenous protein within brain that is not an artifact of antibody cross-reactivity.

Our work is the first, to our knowledge, to examine formation of alpha-synuclein inclusions in vivo within neurons of individual animals over time. This chronic imaging demonstrates that inclusions undergo a stage-like maturation starting from early aggregates with disordered morphology alongside normal soluble somatic and nuclear Syn-GFP. Over the course of weeks, however, inclusions change to become organized and compacted into mature forms that resemble human cortical pathology in dementia with Lewy bodies. Previous work from cross-sectional studies of human tissue has demonstrated various forms of somatic inclusions that appear less compact than classical Lewy bodies, such as cloud-like inclusions and pale bodies (Dale et al., 1992; Gómez-Tortosa et al., 2000). Several groups have postulated that individual aggregates could undergo progressive compaction along a pathway from diffuse aggregates to more-compact Lewy bodies (Dale et al., 1992; Gómez-Tortosa et al., 2000; Wakabayashi et al., 2013). Alternatively, these structures could reflect distinct parallel pathways (Dale et al., 1992). Our work confirms that inclusion maturation can occur in vivo, with progressive compaction as measured by FRAP. It will be important in the future to determine what mechanisms underlie this process.

In parallel with inclusion maturation, we measured a reduction in soluble cytoplasmic and nuclear Syn-GFP in vivo. It is interesting to speculate about the significance of this reduction, because, although a nuclear role for synucleins has been suggested since their initial discovery (Maroteaux et al., 1988), it is less well understood. Specific activities involving intranuclear alpha-synuclein have been recently proposed (Desplats et al., 2011; Liu et al., 2011; Ma et al., 2014), and it may be that loss of nuclear alpha-synuclein when inclusions mature contributes to cellular dysfunction through a loss-of-function mechanism. This would be in parallel to the better-established toxic, gain-of-function consequences of alpha-synuclein aggregation.

Our work strongly suggests that inclusion-bearing neurons selectively degenerate over the course of months, whereas non inclusion-bearing neurons that express soluble Syn-GFP have a much-lower rate of degeneration. This addresses a critical question in the field about the relationship between Lewy pathology formation in individual neurons and their ultimate fate. Although it is clear that Lewy pathology is found in regions where progressive cell death occurs (Fearnley and Lees 1991; Parkkinen et al., 2011; Figure 4G), different models have been proposed (Figure 4H), including ones where Lewy pathology is associated with death of the containing cell (Lu et al., 2005; Greffard et al., 2010), or the opposite, where Lewy pathology is associated with sparing of cell (Gertz et al., 1994; Bodner et al., 2006; Tanaka et al., 2004). Our work suggests that the former model is correct and that Lewy pathology formation is strongly associated with degeneration of the inclusion-bearing cell and not protection (Figure 4H). This argues that Lewy pathology formation itself could play an intimate role in neuronal cell loss, but more work is needed to test this hypothesis, including methods to selectively label the subgroup of neurons that take up PFFs. This could be used to determine what fraction of neurons that take up PFFs go on to form Lewy pathology. Then, by manipulating Lewy pathology to increase or decrease its formation, it should be possible to test whether the statistical association that we have measured for the first time in vivo is due to a causal role for Lewy pathology in cell death or whether more-complicated mechanisms are at play and inclusion formation is actually protective or simply neutral. The injection of other forms of alpha-synuclein (e.g., monomeric and non-fibrillar aggregates) and other amyloidogenic proteins (e.g., tau and beta-amyloid) to test their ability to seed Lewy pathology formation is also of interest for future work in this system, where potential cross-seeding can be studied in individual neurons in vivo.

Overall, our work demonstrates that PFFs can seed progressive conversion of endogenous alpha-synuclein into neuronal inclusions that bear the hallmarks of human disease and lead to selective neuronal degeneration. This system provides a new, in vivo model for testing mechanisms of alpha-synuclein inclusion formation, neuronal cell loss, and potential pathways to halt neurodegeneration in clinically important synucleinopathies.

EXPERIMENTAL PROCEDURES

Animals

Syn-GFP (PDNG78; Rockenstein et al., 2005) heterozygous male mice were mated to BDF1 females (Charles River Laboratories) and housed by OHSU's DCM. Animals were held in a light-dark cycle and temperature- and humidity-controlled vivarium and maintained under ad libitum food and water diet. All experiments were approved by the OHSU IACUC, and every effort was made to minimize the number of animals used and their suffering.

Humans

Human subjects were seen in the Oregon Alzheimer's Disease Center (ADC), and affected subjects had established clinical diagnosis of dementia. Brain autopsy from three patients diagnosed with dementia with Lewy bodies between the ages of 68 and 79 years and three age-matched control cases without clinical evidence of neurodegenerative disease was performed in the ADC neuropathology core. Tissue use was approved by the IRB at OHSU.

Intracerebral Injections and Immunohistochemistry

2- to 3-month-old Syn-GFP mice were injected with mouse WT sequence PFFs, with PBS, or were uninjected controls. Injections were done according to published protocols for PFF generation and preparation (Luk et al., 2012b) and sensory cortex injections (Kuchibhotla et al., 2008). Briefly, 2.5 μl

(2 mg/ml) freshly sonicated PFFs or 2.5 μl PBS was injected into right hemisphere primary sensory in isoflurane (1% to 2%)-anesthetized animals. For IHC studies, whole brains were dissected and the cerebellum removed. Brains were prepared and imaged using published protocols (Spinelli et al., 2014). Briefly, hemispheres were placed in scintillation vials with 4% paraformaldehyde and fixed using a BioWave (Pelco) microwave fixation system. Hemispheres were postfixed in 4% paraformaldehyde overnight at 4°C and then stored in PBS containing sodium azide (0.05%) until use. pSer129 aSyn (81A; 1:667 dilution; Waxman and Giasson, 2008), ubiquitin (Z0458; 1:200 dilution; Dako), and GFP (AB6556; 1:500 dilution; Abcam) primary antibodies were diluted in blocking buffer and slices incubated overnight at 4°C. Appropriate secondary antibodies (Alexa Fluor 647, Alex Fluor 555; 1:1,000; Invitrogen) were incubated overnight at 4°C. Thioflavin S and X-34 staining was performed using standard techniques (Styren et al., 2000). Brain slices were mounted in CFM-2 (Ted Pella), sealed with CoverGrip (Biotium), and allowed to dry overnight in the dark. For confocal imaging, sections were imaged on a Zeiss LSM710 confocal microscope with a Plan-Apochromat 63×/1.40 oil objective. Fluorescence images were analyzed in Fiji (Schindelin et al., 2012) or ImageJ (NIH) with only linear scaling of pixel values. Human neuropathological analysis was done using standard hematoxylin methods. Standard IHC methods were used to evaluate serine-129-phosphorylated alpha-synuclein. In brief, formalin-fixed, paraffin-embedded sections of frontal cortex were incubated with antibody EP1536Y (1:10,000; Abcam), developed with diaminobenzidine chromagen, and counterstained with hematoxylin, as previously described (Leverenz et al., 2008).

Cranial Window Surgery and Imaging

Starting at 2 months post-injection, cranial window surgery was performed and in vivo imaging and photobleaching begun similar to published protocols (Spinelli et al., 2014). Isoflurane-anesthetized animals were placed in a custom-built stereotaxic frame and surgery performed to create an ~5-mm-diameter midline circular craniotomy between bregma and lambda, closed with 8 mm cover glass, and a custom-built aluminum fixation bar cemented into place. On imaging days, isoflurane-anesthetized animals were mounted into the stereotaxic frame and imaged using a Zeiss LSM 7MP multiphoton microscope outfitted with dual channel BiG (binary GaAsP) detectors and a Coherent Technologies Chameleon titanium-sapphire femtosecond pulsed laser source (tuned to 860 nm). Zeiss Zen 2011 image acquisition software was used.

Imaging Analysis

Images were analyzed with ImageJ or Fiji (Schindelin et al., 2012) as previously described (Spinelli et al., 2014). Briefly, regions of interest (ROIs) were selected to obtain mean fluorescence values in relevant ROIs. The inhomogeneity index was calculated as the average root-mean-square deviation of the normalized fluorescence signal across a transect of the cell body. FRAP data were analyzed in Prism 5 (GraphPad) to obtain single exponential fits to the recovery time course and the immobile and mobile fractions. For chronic inclusion imaging >1 day, individual bleached ROI intensities were normalized to unbleached regions to control for possible differences in imaging conditions present on different days.

Statistics

All data are reported as the mean ± SD. Numbers and statistical tests used are reported in relevant sections.

SUPPLEMENTAL INFORMATION

Supplemental Information includes two figures and can be found with this article online at http://dx.doi.org/10.1016/j.celrep.2015.01.060.

AUTHOR CONTRIBUTIONS

V.R.O., K.J.S., and V.K.U. designed the study, performed the mouse experiments, interpreted the results, and wrote the paper. L.J.W. performed the mouse experiments and interpreted the results. K.C.L. provided critical reagents, expertise, interpreted the results, and wrote the paper. R.L.W. performed the human pathological experiments, interpreted the results, and wrote the paper.

ACKNOWLEDGMENTS

We thank Jonathan Taylor for help with mouse colony management; Douglas Zeppenfeld and Jeffrey Iliff for technical assistance with injections; Edward Rockenstein and Eliezer Masliah for Syn-GFP mice; William Klunk for the gift of X-34; Virginia Lee, John Trojanowski, and Gary Westbrook for helpful discussions; and Tamily Weissman for helpful discussions and assistance with figure generation. This work was supported in part by the NIH (grants NS069625, AG024978, AT002688, AG008017, and NS061800) and the Pacific Northwest Parkinson's Group.

Received: September 24, 2014
Revised: December 22, 2014
Accepted: January 27, 2015
Published: February 26, 2015

REFERENCES

Bodner, R.A., Outeiro, T.F., Altmann, S., Maxwell, M.M., Cho, S.H., Hyman, B.T., McLean, P.J., Young, A.B., Housman, D.E., and Kazantsev, A.G. (2006). Pharmacological promotion of inclusion formation: a therapeutic approach for Huntington's and Parkinson's diseases. Proc. Natl. Acad. Sci. USA *103*, 4246–4251.

Brundin, P., Li, J.Y., Holton, J.L., Lindvall, O., and Revesz, T. (2008). Research in motion: the enigma of Parkinson's disease pathology spread. Nat. Rev. Neurosci. *9*, 741–745.

Dale, G.E., Probst, A., Luthert, P., Martin, J., Anderton, B.H., and Leigh, P.N. (1992). Relationships between Lewy bodies and pale bodies in Parkinson's disease. Acta Neuropathol. *83*, 525–529.

Desplats, P., Spencer, B., Coffee, E., Patel, P., Michael, S., Patrick, C., Adame, A., Rockenstein, E., and Masliah, E. (2011). Alpha-synuclein sequesters Dnmt1 from the nucleus: a novel mechanism for epigenetic alterations in Lewy body diseases. J. Biol. Chem. *286*, 9031–9037.

Fearnley, J.M., and Lees, A.J. (1991). Ageing and Parkinson's disease: substantia nigra regional selectivity. Brain *114*, 2283–2301.

Fraser, P.E. (2014). Prions and prion-like proteins. J. Biol. Chem. *289*, 19839–19840.

Gertz, H.J., Siegers, A., and Kuchinke, J. (1994). Stability of cell size and nucleolar size in Lewy body containing neurons of substantia nigra in Parkinson's disease. Brain Res. *637*, 339–341.

Golde, T.E., Borchelt, D.R., Giasson, B.I., and Lewis, J. (2013). Thinking laterally about neurodegenerative proteinopathies. J. Clin. Invest. *123*, 1847–1855.

Gómez-Tortosa, E., Newell, K., Irizarry, M.C., Sanders, J.L., and Hyman, B.T. (2000). alpha-Synuclein immunoreactivity in dementia with Lewy bodies: morphological staging and comparison with ubiquitin immunostaining. Acta Neuropathol. *99*, 352–357.

Greffard, S., Verny, M., Bonnet, A.M., Seilhean, D., Hauw, J.J., and Duyckaerts, C. (2010). A stable proportion of Lewy body bearing neurons in the substantia nigra suggests a model in which the Lewy body causes neuronal death. Neurobiol. Aging *31*, 99–103.

Guo, J.L., and Lee, V.M. (2014). Cell-to-cell transmission of pathogenic proteins in neurodegenerative diseases. Nat. Med. *20*, 130–138.

Jucker, M., and Walker, L.C. (2013). Self-propagation of pathogenic protein aggregates in neurodegenerative diseases. Nature *501*, 45–51.

Kuchibhotla, K.V., Goldman, S.T., Lattarulo, C.R., Wu, H.Y., Hyman, B.T., and Bacskai, B.J. (2008). Abeta plaques lead to aberrant regulation of calcium homeostasis in vivo resulting in structural and functional disruption of neuronal networks. Neuron *59*, 214–225.

Leverenz, J.B., Hamilton, R., Tsuang, D.W., Schantz, A., Vavrek, D., Larson, E.B., Kukull, W.A., Lopez, O., Galasko, D., Masliah, E., et al. (2008). Empiric

refinement of the pathologic assessment of Lewy-related pathology in the dementia patient. Brain Pathol. *18*, 220–224.

Liu, X., Lee, Y.J., Liou, L.C., Ren, Q., Zhang, Z., Wang, S., and Witt, S.N. (2011). Alpha-synuclein functions in the nucleus to protect against hydroxyurea-induced replication stress in yeast. Hum. Mol. Genet. *20*, 3401–3414.

Lu, L., Neff, F., Alvarez-Fischer, D., Henze, C., Xie, Y., Oertel, W.H., Schlegel, J., and Hartmann, A. (2005). Gene expression profiling of Lewy body-bearing neurons in Parkinson's disease. Exp. Neurol. *195*, 27–39.

Luk, K.C., Kehm, V.M., Zhang, B., O'Brien, P., Trojanowski, J.Q., and Lee, V.M. (2012a). Intracerebral inoculation of pathological α-synuclein initiates a rapidly progressive neurodegenerative α-synucleinopathy in mice. J. Exp. Med. *209*, 975–986.

Luk, K.C., Kehm, V., Carroll, J., Zhang, B., O'Brien, P., Trojanowski, J.Q., and Lee, V.M. (2012b). Pathological α-synuclein transmission initiates Parkinson-like neurodegeneration in nontransgenic mice. Science *338*, 949–953.

Ma, K.L., Song, L.K., Yuan, Y.H., Zhang, Y., Yang, J.L., Zhu, P., and Chen, N.H. (2014). α-Synuclein is prone to interaction with the GC-box-like sequence in vitro. Cell. Mol. Neurobiol. *34*, 603–609.

Maroteaux, L., Campanelli, J.T., and Scheller, R.H. (1988). Synuclein: a neuron-specific protein localized to the nucleus and presynaptic nerve terminal. J. Neurosci. *8*, 2804–2815.

Masuda-Suzukake, M., Nonaka, T., Hosokawa, M., Oikawa, T., Arai, T., Akiyama, H., Mann, D.M., and Hasegawa, M. (2013). Prion-like spreading of pathological α-synuclein in brain. Brain *136*, 1128–1138.

Parkkinen, L., O'Sullivan, S.S., Collins, C., Petrie, A., Holton, J.L., Revesz, T., and Lees, A.J. (2011). Disentangling the relationship between lewy bodies and nigral neuronal loss in Parkinson's disease. J Parkinsons Dis *1*, 277–286.

Rockenstein, E., Schwach, G., Ingolic, E., Adame, A., Crews, L., Mante, M., Pfragner, R., Schreiner, E., Windisch, M., and Masliah, E. (2005). Lysosomal pathology associated with alpha-synuclein accumulation in transgenic models using an eGFP fusion protein. J. Neurosci. Res. *80*, 247–259.

Sacino, A.N., Brooks, M., Thomas, M.A., McKinney, A.B., McGarvey, N.H., Rutherford, N.J., Ceballos-Diaz, C., Robertson, J., Golde, T.E., and Giasson, B.I. (2014a). Amyloidogenic α-synuclein seeds do not invariably induce rapid, widespread pathology in mice. Acta Neuropathol. *127*, 645–665.

Sacino, A.N., Brooks, M., Thomas, M.A., McKinney, A.B., Lee, S., Regenhardt, R.W., McGarvey, N.H., Ayers, J.I., Notterpek, L., Borchelt, D.R., et al. (2014b). Intramuscular injection of α-synuclein induces CNS α-synuclein pathology and a rapid-onset motor phenotype in transgenic mice. Proc. Natl. Acad. Sci. USA *111*, 10732–10737.

Sacino, A.N., Brooks, M., McKinney, A.B., Thomas, M.A., Shaw, G., Golde, T.E., and Giasson, B.I. (2014c). Brain injection of α-synuclein induces multiple proteinopathies, gliosis, and a neuronal injury marker. J. Neurosci. *34*, 12368–12378.

Schindelin, J., Arganda-Carreras, I., Frise, E., Kaynig, V., Longair, M., Pietzsch, T., Preibisch, S., Rueden, C., Saalfeld, S., Schmid, B., et al. (2012). Fiji: an open-source platform for biological-image analysis. Nat. Methods *9*, 676–682.

Spinelli, K.J., Taylor, J.K., Osterberg, V.R., Churchill, M.J., Pollock, E., Moore, C., Meshul, C.K., and Unni, V.K. (2014). Presynaptic alpha-synuclein aggregation in a mouse model of Parkinson's disease. J. Neurosci. *34*, 2037–2050.

Styren, S.D., Hamilton, R.L., Styren, G.C., and Klunk, W.E. (2000). X-34, a fluorescent derivative of Congo red: a novel histochemical stain for Alzheimer's disease pathology. J. Histochem. Cytochem. *48*, 1223–1232.

Tanaka, M., Kim, Y.M., Lee, G., Junn, E., Iwatsubo, T., and Mouradian, M.M. (2004). Aggresomes formed by alpha-synuclein and synphilin-1 are cytoprotective. J. Biol. Chem. *279*, 4625–4631.

Unni, V.K., Weissman, T.A., Rockenstein, E., Masliah, E., McLean, P.J., and Hyman, B.T. (2010). In vivo imaging of alpha-synuclein in mouse cortex demonstrates stable expression and differential subcellular compartment mobility. PLoS ONE *5*, e10589.

Volpicelli-Daley, L.A., Luk, K.C., Patel, T.P., Tanik, S.A., Riddle, D.M., Stieber, A., Meaney, D.F., Trojanowski, J.Q., and Lee, V.M. (2011). Exogenous α-synuclein fibrils induce Lewy body pathology leading to synaptic dysfunction and neuron death. Neuron *72*, 57–71.

Wakabayashi, K., Tanji, K., Odagiri, S., Miki, Y., Mori, F., and Takahashi, H. (2013). The Lewy body in Parkinson's disease and related neurodegenerative disorders. Mol. Neurobiol. *47*, 495–508.

Waxman, E.A., and Giasson, B.I. (2008). Specificity and regulation of casein kinase-mediated phosphorylation of alpha-synuclein. J. Neuropathol. Exp. Neurol. *67*, 402–416.